

DOI: 10.1002/cvde.200706596

## Full Paper

# Growth of Hafnium Dioxide Thin Films by MOCVD Using a New Series of Cyclopentadienyl Hafnium Compounds\*\*

By Giovanni Carta,\* Naida El Habra, Gilberto Rossetto, Giacomo Torzo, Laura Crociani, Marco Natali, Pierino Zanella, Gianni Cavinato, Valentina Matterello, Valentino Rigato, Saulius Kaciulis, and Alessio Mezzi

Thin films of  $\text{HfO}_2$  are grown by metal-organic (MO)CVD on Si(001) and fused quartz substrates in the temperature range 400–500 °C, using a new series of bis-cyclopentadienyl bis-amino-alkoxide hafnium precursors, namely  $[(\text{C}_5\text{H}_5)_2\text{Hf}\{\text{OC}(\text{CH}_3)_2\text{CH}_2\text{N}(\text{CH}_3)_2\}_2]$  and  $[(\text{C}_5\text{H}_5)_2\text{Hf}\{\text{OCH}(\text{CH}_3)\text{CH}_2\text{N}(\text{CH}_3)_2\}_2]$ , stable in air because of their strong coordination to the metal center. The films obtained are investigated by X-ray diffraction (XRD), X-ray photoelectron spectroscopy (XPS), Rutherford backscattering spectroscopy (RBS), and atomic force microscopy (AFM). Monoclinic phase  $\text{HfO}_2$  (*baddeleyite*) films, characterized by a correct stoichiometric ratio and a granular surface morphology with a roughness/thickness ratio that decreases with increasing deposition rate, are obtained.

Keywords: Cyclopentadienyl precursors, Hafnia coatings, MOCVD, Polycrystalline films

## 1. Introduction

Thin films of hafnium dioxide ( $\text{HfO}_2$ ) have many important technological applications such as protective coatings,<sup>[1]</sup> mirrors,<sup>[2]</sup> and sensors.<sup>[3]</sup> In particular  $\text{HfO}_2$ , due to the high quality dielectric properties of its polycrystalline films, its high permittivity and stability in contact with silicon, its high density, high heat of formation, and relatively large band gap, has been extensively studied as a replacement for  $\text{SiO}_2$  as the gate-oxide insulating material for sub-0.1  $\mu\text{m}$  complementary metal oxide semiconductor (CMOS) devices.<sup>[4]</sup> These materials are also of interest as insulating dielectrics in the capacitive elements in many memory devices such as DRAM, and in thin-film electroluminescent (TFEL) applications.<sup>[5]</sup>

$\text{HfO}_2$  thin films have been prepared by several techniques such as physical vapor deposition (PVD),<sup>[6]</sup> atomic

layer deposition (ALD),<sup>[7]</sup> sol-gel processes,<sup>[8]</sup> and MOCVD.<sup>[9]</sup> In particular, the MOCVD process offers the potential for large area growth, good conformal step coverage even on non-planar device geometries, great versatility, and the possibility of carrying out film deposition at relatively low temperatures. Nevertheless, one of the fundamental requirements is the availability of precursors with an adequate volatility for an efficient vapor phase transport. Up to date, the compounds that have been largely employed as precursors for  $\text{HfO}_2$  thin film deposition include  $\text{HfCl}_4$ ,<sup>[10]</sup>  $\beta$ -diketonates and their fluorinated complexes,<sup>[11]</sup>  $\text{Hf}(\text{NO}_3)_4$ ,<sup>[12]</sup> and  $\text{Hf}(\text{NEt}_2)_4$ ,<sup>[13]</sup> even if they present some drawbacks such as a low volatility, high evaporation and deposition temperatures, heavy carbon and fluorine contamination of the deposits, and great air and moisture sensitivity.

Other useful compounds that have been employed are the tetra-alkoxide complexes which, however, present the problem of oligomerization which reduces their volatility. Nevertheless, the presence of bulky ligands on the molecular skeleton inhibits oligomerization, thus allowing  $\text{Hf}(\text{O}^i\text{Bu})_4$  to be successfully employed for the deposition of oxide layers,<sup>[14]</sup> even though it presents the drawback of containing an unsaturated four-coordinate metal center which makes it very reactive to air and moisture.

Recently, new hafnium homoleptic alkoxide compounds fully saturated, such as  $\text{Hf}(\text{dmae})_4$  ( $\text{dmae}$  = dimethylaminoethoxide)<sup>[15]</sup> and  $\text{Hf}(\text{mmp})_4$  ( $\text{mmp}$  = 1-methoxy-2-methyl-2-propanolate),<sup>[16]</sup> and heteroleptic complexes such as  $\text{Hf}(\text{O}^i\text{Bu})_2(\text{mmp})_2$ ,<sup>[17]</sup> and  $\text{Hf}(\text{O}^i\text{Pr})_2(\text{tbaoac})_2$  ( $\text{tbaoac}$  = *tert*-butylacetoacetato),<sup>[18]</sup> have been successfully used as they simultaneously inhibit oligomerization and increase the coordination number of the central metal. Moreover,

[\*] Dr. G. Carta, Dr. N. El Habra, Dr. G. Rossetto, Prof. G. Torzo, Dr. L. Crociani, Dr. M. Natali, Dr. P. Zanella  
CNR-ICIS, C.so Stati Uniti, 4 35127 Padova (Italy)  
E-mail: carta@icis.cnr.it

Prof. G. Cavinato  
Dipartimento di Scienze Chimiche, Università di Padova  
Via Marzolo, 1, 35131 Padova (Italy)

Dr. V. Matterello, Prof. V. Rigato  
INFN, Laboratori Nazionali di Legnaro  
V.le dell'Università 2 35020 Legnaro, Padova (Italy)

Dr. S. Kaciulis, Dr. A. Mezzi  
CNR-ISMN, P.O. Box 10  
00016 Monterotondo Stazione (RM) (Italy)

[\*\*] The authors wish to thank Mr. Valerio Corrado for technical assistance and Mrs. Anna Moresco for elemental analysis.

the tetrahydroxydiethylamide,  $\text{Hf}(\text{ONEt}_2)_4$ ,<sup>[19]</sup> (more stable than the coordinatively unsaturated  $\text{Hf}(\text{NEt}_2)_4$ ) and multinuclear compounds like  $\text{Hf}_3\text{O}(\text{ONep})_{10}$  (Nep = neopentyl)<sup>[20]</sup> have been investigated and employed.

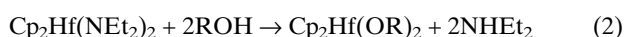
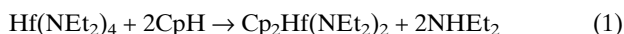
An alternative class of precursors could be represented by the cyclopentadienyl complexes coordinatively saturated with dialkylamide, dialkoxide, and dialkylamino-alkoxide ligands. In previous works, some hafnocene compounds with a series of bicyclo[2.2.1]heptanolates ligands [ $\text{Cp}_2\text{Hf}(\text{OBL})_2$ ,  $\text{Cp}_2\text{Hf}(\text{ONBL})_2$ ; Cp = cyclopentadienyl, OBL = borneol, ONBL = norborneol],<sup>[21]</sup> with alkyl and dialkylamide moieties [ $\text{Cp}_2\text{Hf}(\text{L})_2$ , L = Me, N(Me)<sub>2</sub>, N(Et)<sub>2</sub>]<sup>[22]</sup> and, more recently, with dialkoxide and dialkoxy-alkoxide having a different steric hindrance [ $\text{Cp}_2\text{Hf}(\text{OL})_2$ , L = CH(CH<sub>3</sub>)<sub>2</sub>, CH(CH<sub>3</sub>)CH<sub>2</sub>OCH<sub>3</sub>, C(CH<sub>3</sub>)<sub>2</sub>CH<sub>2</sub>OCH<sub>3</sub>, C(CH<sub>2</sub>CH<sub>3</sub>)<sub>2</sub>CH<sub>2</sub>OCH<sub>3</sub>],<sup>[23]</sup> have been investigated and used successfully.

In this work, a new series of bis-cyclopentadienyl bis-amino-alkoxide precursors, namely bis(cyclopentadienyl)bis(1-dimethylamino-2-methyl-2-propoxy)hafnium(IV) [(C<sub>5</sub>H<sub>5</sub>)<sub>2</sub>-Hf{OC(CH<sub>3</sub>)<sub>2</sub>CH<sub>2</sub>N(CH<sub>3</sub>)<sub>2</sub>}<sub>2</sub>] (**1**) and bis(cyclopentadienyl)bis(1-dimethylamino-2-propoxy)hafnium(IV) [(C<sub>5</sub>H<sub>5</sub>)<sub>2</sub>-Hf{OCH(CH<sub>3</sub>)CH<sub>2</sub>N(CH<sub>3</sub>)<sub>2</sub>}<sub>2</sub>] (**2**) have been synthesized, characterized by nuclear magnetic resonance (NMR) spectroscopy and used as MOCVD precursors for the growth of HfO<sub>2</sub> thin films. The deposits, obtained on fused quartz and Si(001) substrates, were analyzed using XRD, XPS, RBS, and AFM.

## 2. Results and Discussion

### 2.1. Precursors Synthesis and Characterization

Hafnium(IV) complexes **1** and **2** were obtained by a simple two-step procedure using the following general Reactions 1 and 2 in conformity with the known displacement order  $\text{R} < \text{NR}_2 < \text{Cp} < \text{OR}$ <sup>[24]</sup> giving air-stable products in good yields (80–90 %) and purity.



Cp = cyclopentadienyl, Et = ethyl, R = –C(CH<sub>3</sub>)<sub>2</sub>CH<sub>2</sub>N(CH<sub>3</sub>)<sub>2</sub>, –CH(CH<sub>3</sub>)CH<sub>2</sub>N(CH<sub>3</sub>)<sub>2</sub>. As already reported in the literature,<sup>[16]</sup> and also in this case, the <sup>1</sup>H and <sup>13</sup>C NMR distortionless enhancement by polarization transfer (DEPT) peaks of these complexes in deuterated benzene

solution did not show any evidence of line broadening, thus indicating that molecules were not fluxional and, probably, mononuclear in solution being oligomerization-inhibited by the steric hindrance of the two cyclopentadienyl groups and by the two amino-alkoxide ligands. Unfortunately, as no crystal structure has been obtained, it can be argued that these precursors present a molecular structure coordinatively saturated at the metal center, consistent with their high stability in air.

### 2.2. MOCVD of HfO<sub>2</sub> Thin Films

Thin films of hafnia with various thicknesses were grown using **1** and **2** as precursors in an atmosphere of oxygen mixed with water vapor as the reactant gas, as H<sub>2</sub>O molecules favor the hydrolytic cleavage of the organic moieties giving stable leaving species, thus reducing the carbon contamination within the films.<sup>[25]</sup> The experimental conditions are reported in Table 1. The obtained films were colorless and well adherent to the substrate with a uniform, crack-free surface. It is worthwhile noticing that the two precursors show a different, singular behavior; films grown using precursor **1** present a growth rate that increases with temperature, while those obtained from precursor **2** show a reverse order. This is probably due to the different thermal stability of the two precursors. In fact, precursor **2**, more volatile but less thermally stable than precursor **1**, shows the highest growth rate at the lowest investigated temperature. At higher temperatures (> 400 °C), it thermally decomposes in the homogeneous gas phase giving a lower growth rate, while precursor **1**, more thermally stable, possesses the higher deposition rate. This is also confirmed from preliminary thermogravimetric measurements under a N<sub>2</sub> atmosphere. Precursor **2** starts its sublimation process at 120 °C and finishes at 190 °C; then, at 430 °C it underwent a further mass loss up to 600 °C, presumably due to its decomposition generating a residue that remains stable up to 1000 °C. Precursor **1** is less volatile as it starts to lose mass at 140 °C and finishes at 200 °C, corresponding to a sublimation process, giving a small quantity of a residue that remains stable up to 1000 °C.

Film microstructure was investigated by XRD analysis showing that all the films grown with the two precursors, both on Si(001) and fused quartz substrates, were polycrystalline with a monoclinic (*baddeleyite*) HfO<sub>2</sub> structure (ICDD pattern 01–078–0050). In Figure 1, the XRD patterns of the films grown at 450 °C on Si(001) with the two precursors, are shown. The sample grown with precursor **1**

Table 1. Experimental growth conditions for HfO<sub>2</sub> thin films, using N<sub>2</sub> as the carrier gas (125 sccm) and oxygen mixed with water vapor (250 sccm) as the reactant gas.

Precursor	Evap. temp. [°C]	Growth temp. [°C]	P [Torr]	Dep. Time [min]	Thickn. [nm]	Growth rate [nm min <sup>-1</sup> ]
$\text{Cp}_2\text{Hf}(\text{OC}(\text{CH}_3)_2\text{CH}_2\text{N}(\text{CH}_3)_2)_2$ ( <b>1</b> )	160	400, 450, 500	4.2	30	110, 120, 150	3.66, 4.0, 5.0
$\text{Cp}_2\text{Hf}(\text{OCH}(\text{CH}_3)\text{CH}_2\text{N}(\text{CH}_3)_2)_2$ ( <b>2</b> )	140	400, 450, 500	4.2	30	120, 70, 60	4.0, 2.33, 2.0

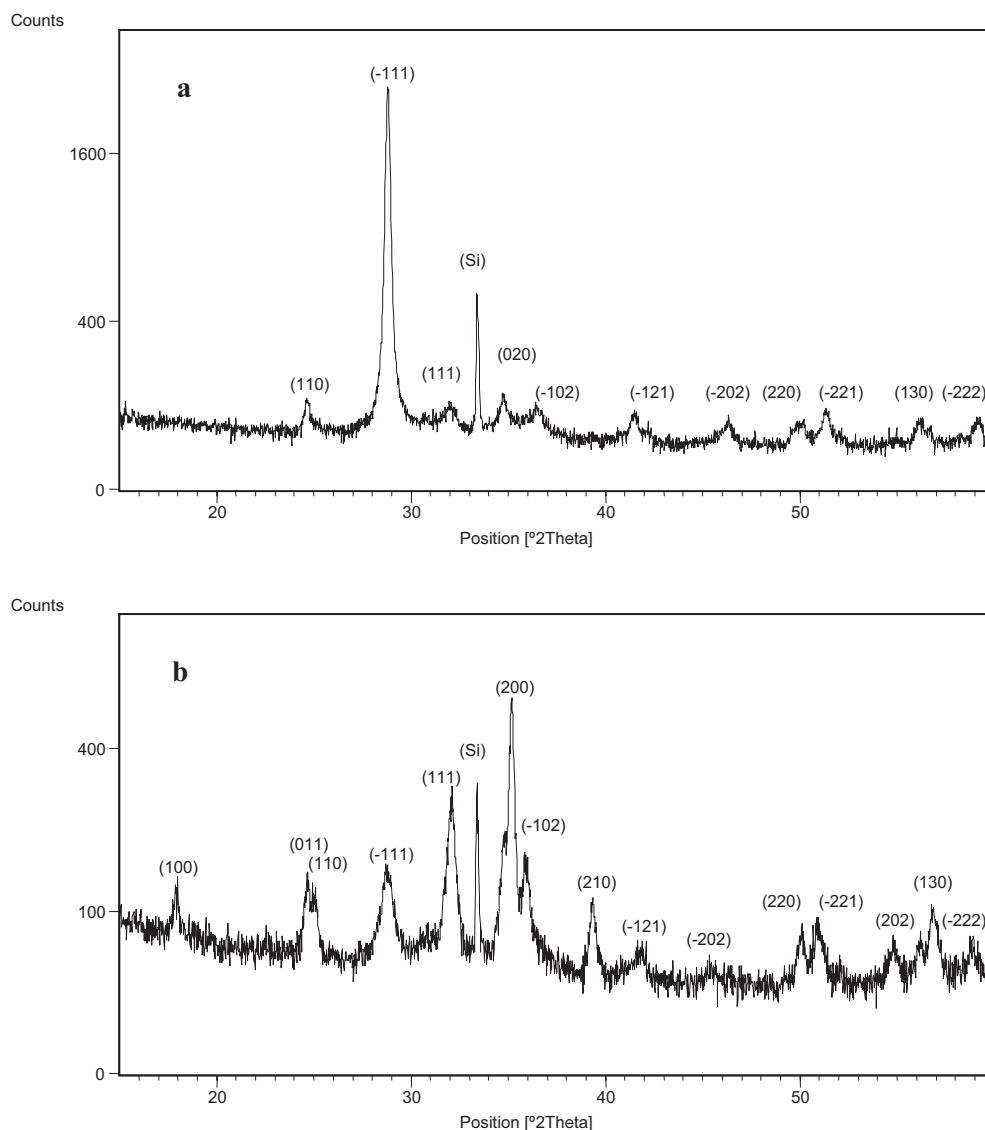


Fig. 1. XRD patterns of HfO<sub>2</sub> thin films grown using a) **1**, and b) **2** at 450 °C on Si(001) substrates.

(Fig. 1a), showed a (-111) preferential orientation independent of the growth temperature. The average crystallite size, estimated from the analysis of the most intense signal, increased progressively from 38 to 52 nm with a temperature increase from 400 to 500 °C. At variance with that, films grown with precursor **2** showed both at 500 °C (crystallite size = 84 nm) and at 450 °C (crystallite size = 42 nm) a (200) preferential orientation, while at 400 °C, the XRD peaks were hardly detectable. A common characteristic for all the films obtained with the two precursors is that the crystallite grain size increased with temperature. Such behavior might be due to a temperature effect which increases the crystal grain mobility at the same time as favoring their ordered arrangement during the growth.

The chemical composition and the purity of the deposited films were determined by XPS analysis. The Hf 4f spectrum, similar for all the films obtained with the two

precursors on both the substrates, showed that the main Hf 4f<sub>7/2</sub> peak had a value of binding energy BE 16.8 eV (Fig. 2). This BE value, within the margins of experimental error, confirms that hafnium is in the +4 oxidation state and corresponds to HfO<sub>2</sub> films.<sup>[26]</sup> Also, the low full width at half maximum (FWHM) values (1.4–1.5 eV) of synthetic Hf 4f peaks, obtained by XPS peak-fitting routine, and the correct area ratio (4:3) of these peaks, testified to the presence of single-phase HfO<sub>2</sub>.

A compositional depth profile, determined from XPS data for the sample grown at 500 °C on fused quartz using precursor **1**, is shown in Figure 3. As can be seen, the superficial carbon contamination is reduced from 30 % to 20 % after a short sputtering time that corresponds to a 0.2 nm depth (due to the large sputtered area, Ar<sup>+</sup> sputtering rate was about 0.01 nm min<sup>-1</sup>). The residual carbon contamination in the bulk layer, remaining constant through the

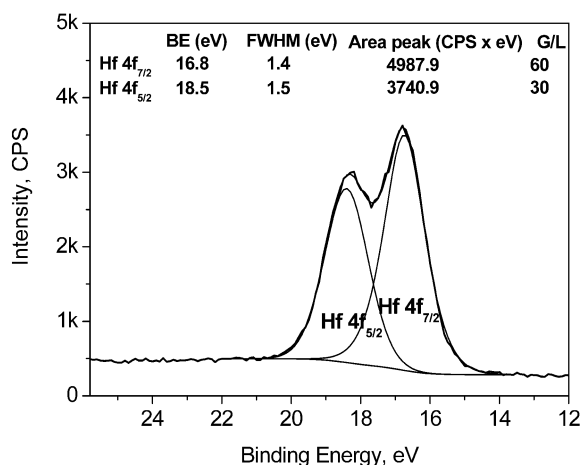


Fig. 2. XPS spectrum of Hf 4f region of the HfO<sub>2</sub> film deposited at 500 °C on fused quartz, using precursor 1.

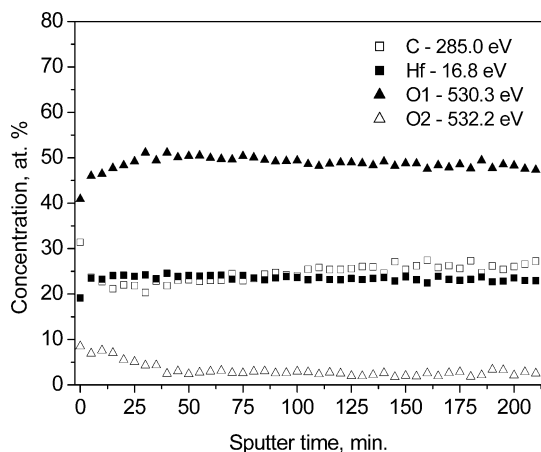


Fig. 3. XPS depth profile (Ar<sup>+</sup>, 2.0 keV) of the HfO<sub>2</sub> film deposited at 500 °C on fused quartz, using precursor 1.

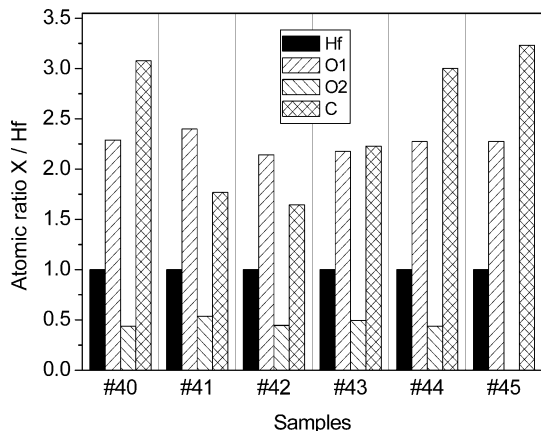


Fig. 4. Relative surface composition (normalized to Hf concentration) of the as-deposited samples (i.e., before sputtering): samples #40–42 grown from precursor 1; #43–45 grown from precursor 2. Growth temperatures: #40, 43 at 400 °C; #41, 44 at 450 °C; #42, 45 at 500 °C.

thickness of the film, is characterized by C 1s peak at BE = 285.0 eV (C–C and/or C–H bonds) and, together with the low contribution of hydroxyl groups (O 1s peak marked O2 at BE 532.2 eV), it can be explained as an organic residue coming from an incomplete precursor decomposition during the MOCVD process. The atomic ratio of oxygen (O 1s peak at BE 530.3 eV) and hafnium is about 2:1 through the whole depth profile, thus indicating that the oxide is stoichiometric. Relative surface composition (normalized to Hf concentration) of different samples before

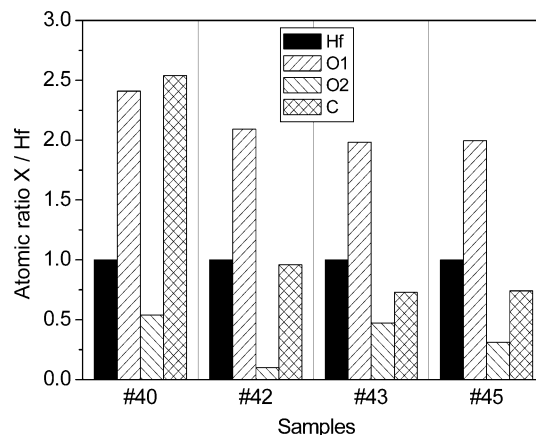


Fig. 5. Relative chemical compositions (normalized to Hf concentration) of four samples after 100 min of Ar<sup>+</sup> sputtering (depth ~ 1 nm). Sample numbering is the same as that reported in Fig. 4.

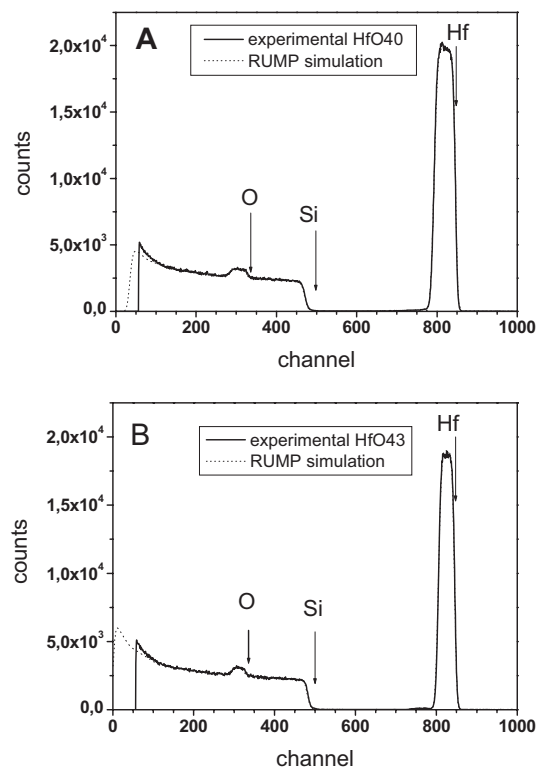


Fig. 6. RBS spectra of the samples grown at 400 °C on Si(001) using precursor a) 1 and b) 2 respectively.



sputtering (i.e., as-deposited), grown using precursor **1** (samples #40–42) and precursor **2** (samples #43–45), is reported in Figure 4, while the composition of four samples (samples #40, 42 and 43, 45) after 100 min of  $\text{Ar}^+$  sputtering (depth =  $\sim 1$  nm) is reported in Figure 5. In both the Figures (i.e., before and after sputtering), the atomic ratio O/Hf in the oxides changes from 2 to 2.4, probably due to the presence of super-stoichiometric species which contain an excess of oxygen. These variable O/M ratios are a common feature in metal-oxide films deposited by MOCVD from many precursors. The comparison of contamination on the surface and on the bulk layer of the films (C and O<sub>2</sub> in Figs. 4 and 5) indicates that, for the samples grown with precursor **1**, the carbon concentration decreases both on the surface and in the bulk, with rising temperature, while for those deposited employing precursor **2** the carbon contamination on the surface seems to increase together with the growth temperature, while in the bulk it remains constant, independent of the growth temperature (Fig. 5 samples #43 and 45, deposited at 400 and 500 °C, respectively). This indicates that, in the latter case, the different carbon contamination strongly depends on the sample handling and not on the experimental conditions used, and that the less thermal stability of **2**, as previously discussed, gives a low carbon incorporation within the film, which it is not influenced by varying the temperature. On the contrary, precursor **1** being more thermally stable at low temperatures, it does not completely react leaving more carbonaceous residues incorporated in the bulk of the film.

It can be seen, therefore, that while the optimal growth using precursor **1** takes place at the highest growth temperature, as there is both the lowest carbon contamination and the highest growth rate (sample #42 deposited at 500 °C), when using precursor **2** it is preferable to grow at 400 °C because, even though the carbon contamination within the bulk is very similar, the growth rate is highest at this temperature.

Typical RBS spectra for films deposited on Si(001) using precursors **1** and **2** are shown in Figure 6. Superimposed on the experimental spectra are the simulated curves. The

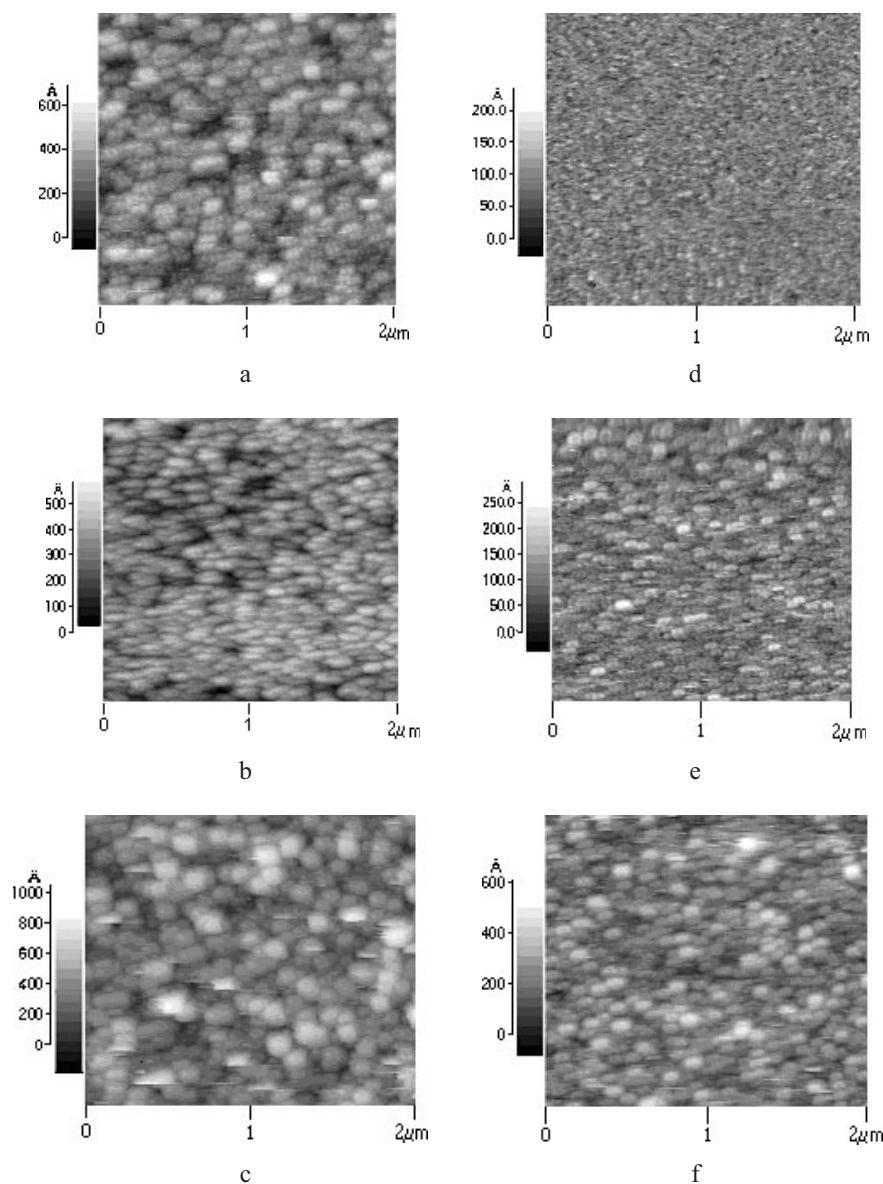


Fig. 7. AFM images ( $2\ \mu\text{m} \times 2\ \mu\text{m}$ ) of the  $\text{HfO}_2$  thin films grown on Si(001) substrate at 400–450–500 °C using (a, b, c) precursor **1** and (d, e, f) **2**, respectively.

edges of the Si, Hf, and O signals can be clearly seen. The stoichiometry of the films obtained from the simulations is very close to  $\text{HfO}_2$  with a O/Hf ratio in the range 2.03–2.22, in qualitative agreement with the XPS values. RBS spectra allowed the determination of film thickness by using the known density of the monoclinic  $\text{HfO}_2$  phase, that is  $10.1\ \text{g cm}^{-3}$ , obtaining thickness values very close to those measured by the profiler.

Film surface morphology was investigated using AFM. Representative images in a  $2\ \mu\text{m} \times 2\ \mu\text{m}$  area of films deposited on Si(001) at the three investigated temperatures, using the two precursors, are reported in Figure 7. The films presented a granular morphology with root mean square (rms) roughness values at 400, 450, and 500 °C which were 7.74 Å, 5.14 Å, 2.91 Å, respectively, for sam-

ples obtained from precursor **1** and 1.22 Å, 0.70 Å, and 1.16 Å respectively, for samples obtained from precursor **2**. Dividing the rms by the film thickness ( $t$ ), rms/ $t$  ratios of  $0.070 \pm 0.002$ ,  $0.043 \pm 0.002$ , and  $0.019 \pm 0.002$  were obtained for samples grown with precursor **1**, while for samples obtained from precursor **2** the respective values were  $0.010 \pm 0.002$ ,  $0.010 \pm 0.002$ , and  $0.019 \pm 0.002$ . Similar behavior can be detected for all the films; the rms/ $t$  ratio decreases with increasing deposition rate (see Table 1). This suggests that the roughness might be correlated to growth stress in the film that can relax by the formation of agglomerates via surface diffusion, and subsequent aggregation which gives rise to a rugged surface. Therefore, for lower growth rates, there is more time for the atomic species to diffuse and to agglomerate than is the case for higher growth rates where diffusing atoms are blocked by newly deposited atoms which smother the surface as the thickness increases.

### 3. Conclusions

Two new bis-cyclopentadienyl bis-amino-alkoxide hafnium (IV) precursors have been synthesized and characterized by NMR. These complexes, thanks to the presence of bulky ligands that fully saturate the coordination of the metal center, do not present oligomerization and result in greater stability in air compared to the usually employed  $\text{Hf}(\text{O}^i\text{Bu})_4$ . Moreover, they are less volatile than the respective bis-cyclopentadienyl dialkoxide compounds, thus showing a stronger coordinating power of oxy-nitrogen ligands.  $\text{HfO}_2$  thin films grown by MOCVD on Si(001) and fused quartz substrates at three different temperatures are well adherent, colorless, and crack-free. Structural and compositional measurements have shown the formation of monoclinic (*baddeleyite*)  $\text{HfO}_2$  free from undesired phases. All the films are characterized by a granular surface morphology, with a roughness/thickness ratio that decreases with increasing growth rate.

### 4. Experimental

**Precursor Synthesis:** All the reactions were carried out in a dry box under a nitrogen atmosphere. Hafnium(IV) chloride (99.9%) (Strem), and butyllithium (Aldrich), were used without further purification. Fresh cyclopentadiene was obtained from the cracking at 170 °C of dicyclopentadiene (Aldrich) and used at once. Diethylamine and the commercial amino-alcohols (Aldrich) were used after further anhydrication by distillation at room pressure over calcium hydride, n-hexane and toluene over K-benzophenone alloy. The 1-dimethylamino-2-methyl-2-propanol was obtained as reported in literature [27].

$^1\text{H}$  NMR experiments were performed using a Bruker 300 MHz spectrometer with  $\text{C}_6\text{D}_6$  as a solvent. A  $^{13}\text{C}$  NMR DEPT experiment was used with a 135° pulse to distinguish the primary and tertiary carbon atoms from the secondary one.

$[(\text{C}_5\text{H}_5)_2\text{Hf}[\text{OC}(\text{CH}_3)_2\text{CH}_2\text{N}(\text{CH}_3)_2]_2](\textbf{1})$ : To a stirred solution of  $\text{Hf}(\text{NEt}_2)_4$  (obtained by reaction of an excess of  $\text{NH}(\text{CH}_2\text{CH}_3)_2$  with 1.6 M solution of butyllithium in n-hexane and  $\text{HfCl}_4$ ), (2.06 g, 4.41 mmol) in toluene (40 cm<sup>3</sup>), 3 mL of CpH (32.56 mmol) in toluene (20 cm<sup>3</sup>) were added dropwise. The solution was boiled under reflux for 20 h and then the solvent and the amine were removed in vacuo to give the  $\text{Cp}_2\text{Hf}(\text{NEt}_2)_2$  as a yellow

pure solid. To a stirred solution of this product (0.334 g, 0.737 mmol) dissolved in n-hexane (40 cm<sup>3</sup>), 0.440 g (3.76 mmol) of 1-dimethylamino-2-methyl-2-propanol diluted in n-hexane (5 cm<sup>3</sup>) were added slowly dropwise. After 3 days the solvent was removed in vacuo giving **1** as an orange oil. Elem. Anal.: Theor.; C 48.83 %, H 7.08 %, N 5.17 %. Exp.; C 47.87 %, H 7.03 %, N 4.85 %.  $^1\text{H}$  NMR ( $\text{C}_6\text{D}_6$ , 25 °C)  $\delta$  [ppm]: 1.22 (s, 12H,  $[(\text{C}_5\text{H}_5)_2\text{Hf}[\text{OC}(\text{CH}_3)_2\text{CH}_2\text{N}(\text{CH}_3)_2]_2]$ ), 2.16 (s, 4H,  $[(\text{C}_5\text{H}_5)_2\text{Hf}[\text{OC}(\text{CH}_3)_2\text{CH}_2\text{N}(\text{CH}_3)_2]_2]$ ), 2.27 (s, 12H,  $[(\text{C}_5\text{H}_5)_2\text{Hf}[\text{OC}(\text{CH}_3)_2\text{CH}_2\text{N}(\text{CH}_3)_2]_2]$ ), 6.03 (s, 10H,  $[(\text{C}_5\text{H}_5)_2\text{Hf}[\text{OC}(\text{CH}_3)_2\text{CH}_2\text{N}(\text{CH}_3)_2]_2]$ ).  $^{13}\text{C}$  NMR DEPT ( $\text{C}_6\text{D}_6$ , 25 °C)  $\delta$  [ppm]: 28.96  $[(\text{C}_5\text{H}_5)_2\text{Hf}[\text{OC}(\text{CH}_3)_2\text{CH}_2\text{N}(\text{CH}_3)_2]_2]$ , 48.16  $[(\text{C}_5\text{H}_5)_2\text{Hf}[\text{OC}(\text{CH}_3)_2\text{CH}_2\text{N}(\text{CH}_3)_2]_2]$ , 72.14  $[(\text{C}_5\text{H}_5)_2\text{Hf}[\text{OC}(\text{CH}_3)_2\text{CH}_2\text{N}(\text{CH}_3)_2]_2]$ , 110.73  $[(\text{C}_5\text{H}_5)_2\text{Hf}[\text{OC}(\text{CH}_3)_2\text{CH}_2\text{N}(\text{CH}_3)_2]_2]$ .

$[(\text{C}_5\text{H}_5)_2\text{Hf}[\text{OCH}(\text{CH}_3)\text{CH}_2\text{N}(\text{CH}_3)_2]_2](\textbf{2})$ : The complex was synthesized by the dropwise addition of 1-dimethylamino-2-propanol (0.164 g, 1.82 mmol) diluted in n-hexane (5 cm<sup>3</sup>) to a stirred solution of  $\text{Cp}_2\text{Hf}(\text{NEt}_2)_2$  (0.190 g, 0.42 mmol) in n-hexane (40 cm<sup>3</sup>). After 7 days the solvent was removed in vacuo giving **2** as an orange oil. Elem. Anal.: Theor.; C 46.82 %, H 6.68 %, N 5.45 %. Exp.; C 44.35 %, H 6.60 %, N 4.88 %.  $^1\text{H}$  NMR ( $\text{C}_6\text{D}_6$ , 25 °C)  $\delta$  [ppm]: 6.07 (s, 10H,  $[(\text{C}_5\text{H}_5)_2\text{Hf}[\text{OCH}(\text{CH}_3)\text{CH}_2\text{N}(\text{CH}_3)_2]_2]$ ), 4.17 (m, 2H,  $[(\text{C}_5\text{H}_5)_2\text{Hf}[\text{OCH}(\text{CH}_3)\text{CH}_2\text{N}(\text{CH}_3)_2]_2]$ ), 2.20 (s, 12H,  $[(\text{C}_5\text{H}_5)_2\text{Hf}[\text{OCH}(\text{CH}_3)\text{CH}_2\text{N}(\text{CH}_3)_2]_2]$ ), 2.09 (d, 4H,  $[(\text{C}_5\text{H}_5)_2\text{Hf}[\text{OCH}(\text{CH}_3)\text{CH}_2\text{N}(\text{CH}_3)_2]_2]$ ), 1.24 (d, 6H,  $[(\text{C}_5\text{H}_5)_2\text{Hf}[\text{OCH}(\text{CH}_3)\text{CH}_2\text{N}(\text{CH}_3)_2]_2]$ ).  $^{13}\text{C}$  NMR DEPT ( $\text{C}_6\text{D}_6$ , 25 °C)  $\delta$  [ppm]: 26.68  $[(\text{C}_5\text{H}_5)_2\text{Hf}[\text{OCH}(\text{CH}_3)\text{CH}_2\text{N}(\text{CH}_3)_2]_2]$ , 48.51  $[(\text{C}_5\text{H}_5)_2\text{Hf}[\text{OCH}(\text{CH}_3)\text{CH}_2\text{N}(\text{CH}_3)_2]_2]$ , 70.10  $[(\text{C}_5\text{H}_5)_2\text{Hf}[\text{OCH}(\text{CH}_3)\text{CH}_2\text{N}(\text{CH}_3)_2]_2]$ , 73.05  $[(\text{C}_5\text{H}_5)_2\text{Hf}[\text{OCH}(\text{CH}_3)\text{CH}_2\text{N}(\text{CH}_3)_2]_2]$ , 110.69  $[(\text{C}_5\text{H}_5)_2\text{Hf}[\text{OCH}(\text{CH}_3)\text{CH}_2\text{N}(\text{CH}_3)_2]_2]$ .

**Film Growth and Characterization:**  $\text{HfO}_2$  thin films were deposited in a low-pressure, hot-wall MOCVD reactor equipped with a Pyrex tube heated by a tubular furnace. The carrier gas was  $\text{N}_2$  (flow rate = 125 sccm), flowing through a bubbler containing the hafnium precursor thermostatically set to a temperature suitable for an efficient vaporization and thermal stability (160 °C for **1** and 140 °C for **2**). The reactant gas ( $\text{O}_2 + \text{H}_2\text{O}$ ) was introduced in the main flow in the vicinity of the reaction zone, with a flow rate of 250 sccm. Prior to entering the reaction chamber, oxygen was bubbled into a 500 cm<sup>3</sup> flask containing 250 cm<sup>3</sup> of distilled water kept at 30 °C. The amount of released water, 20 g h<sup>-1</sup>, was constant for all of the depositions. For all the experiments, the total pressure was kept at 4.2 Torr, the deposition time was 30 min and the growth temperature ranged from 400 °C to 500 °C. The substrates used were fused quartz and cut polished Si(001) wafers. Prior to each deposition experiment, substrates were cleaned with hot trichloroethylene and rinsed with acetone in order to minimize their surface contamination.

Film thicknesses were determined using a KLA Tencor Alpha-Step IQ surface profiler used to analyze the film height steps on partially masked samples.

XRD spectra were recorded in  $2\theta/\omega$  method using an X'Pert PW 3710 Philips instrument using Cu K $\alpha$  radiation. A parallel plate collimator was used in front of the detector. Phase identification was performed with the support of the standard ICDD files. The average crystallite size was estimated by means of the Scherrer formula.

The XPS analyses were performed using an Escalab Mk II spectrometer, equipped with a standard Al K $\alpha$  excitation source ( $h\nu = 1486.6$  eV) and a five channeltron detection system. The BE scale was calibrated by measuring the C 1s peak (BE = 285.0 eV) from the surface contamination. The accuracy of the measured BE was  $\pm 0.1$  eV. The measurements were conducted under the chamber pressure of about  $1 \times 10^{-7}$  Pa that was increased to  $1 \times 10^{-5}$  Pa during the depth profiling. The energy of the ion gun ( $\text{Ar}^+$ ), used for the depth profiling, was fixed at 2.0 keV. Registered spectra were processed by the CasaXPS v. 2.2.84 software, using a peak-fitting routine with symmetrical Gaussian-Lorentzian functions. Background intensity was subtracted from the photoelectron spectra using the Shirley method.

AFM characterization of surface morphology was performed with a Park Scientific Instrument-Model CP using silicon cantilever tips with nominal curvature radius of 10 nm in contact mode. Images were recorded at various sample areas in order to check surface homogeneity.

RBS spectra were collected at INFN-LNL laboratories (Legnaro, Italy) using the AN 2000 accelerator, with a 2.2 MeV  $\text{He}^{2+}$  beam. Fixed random spectra were recorded and the film stoichiometry and thickness evaluated by simulating the spectra using the RUMP software package. Elemental analyses were performed on a Carlo Erba 1106 Elemental Analyzer.

Received: January 31, 2007

Revised: June 4, 2007

- [1] R. D. Valtiri, F. S. Galasso, German Patent DE 3427911 **1986**.
- [2] W. H. Lowdermilk, d. Milam, F. Rainer, *Thin Solid Films* **1980**, 73, 155.

- [3] V. K. Khanna, R. K. Nahar, *Appl. Surf. Sci.* **1987**, 28, 247.
- [4] G. D. Wilk, R. M. Wallace, J. M. Anthony, *J. Appl. Phys.* **2001**, 89, 5243.
- [5] C. T. Hsu, S. W. Li, C. H. Liu, Y. K. Su, T. S. Wu, M. Yokoyama, *J. Appl. Phys.* **1992**, 71, 1509.
- [6] A. K. Jonsson, G. A. Niklasson, M. Veszelei, *Thin Solid Films* **2002**, 402, 242.
- [7] D. M. Hausmann, E. Kim, J. Becker, R. G. Gordon, *Chem. Mater.* **2002**, 14, 4350.
- [8] T. Nishide, S. Honda, M. Matsuura, M. Ide, *Thin Solid Films* **2000**, 61, 371.
- [9] Y. Ohshita, A. Ogura, A. Hoshino, S. Hihiro, T. Suzuki, H. Mashida, *Thin Solid Films* **2002**, 406, 215.
- [10] C. F. Powell in *Chemically Deposited Nonmetals* (Eds: C. F. Powell, J. H. Oxley, J. M. Blocher), John Wiley & Sons Inc., New York **1966**, p. 343.
- [11] M. Balog, M. Schieber, M. Michman, S. Patai, *Thin Solid Films* **1977**, 41, 247.
- [12] D. G. Colombo, D. C. Gilmer, V. G. Young Jr., S. A. Campbell, W. L. Gladfelter, *Chem. Vap. Deposition* **1998**, 4, 220.
- [13] Y. Ohshita, A. Ogura, A. Hoshino, S. Hihiro, H. Mashida, *J. Cryst. Growth* **2001**, 233, 292.
- [14] K. S. Mazdiyasi, R. T. Dolloff, J. S. Smith, *J. Am. Ceram. Soc.* **1969**, 52, 523.
- [15] M. K. Song, S. W. Kang, S. W. Rhee, *Thin Solid Films* **2004**, 450, 272.
- [16] P. A. Williams, J. L. Roberts, A. C. Jones, P. R. Chalker, N. L. Tobin, J. F. Bickley, H. O. Davies, L. M. Smith, T. J. Leedham, *Chem. Vap. Deposition* **2002**, 8, 163.
- [17] P. A. Williams, J. L. Roberts, A. C. Jones, P. R. Chalker, J. F. Bickley, J. F. Steiner, H. O. Davies, T. J. Leedham, *J. Mater. Chem.* **2002**, 12, 165.
- [18] A. Baunemann, R. Thomas, R. Becker, M. Winter, R. A. Fisher, P. Ehrhart, R. Waser, A. Devi, *Chem. Commun.* **2004**, 1610.
- [19] P. A. Williams, A. C. Jones, N. L. Tobin, P. R. Chalker, S. Taylor, P. A. Marshall, J. F. Bickley, L. M. Smith, H. O. Davies, G. W. Critchlow, *Chem. Vap. Deposition* **2003**, 9, 309.
- [20] A. Abrutis, L. G. Hubert-Pfalzgraf, S. V. Pasko, A. Bartasyte, F. Weiss, V. Janickis, *J. Cryst. Growth* **2004**, 267, 529.
- [21] A. V. Grafov, E. A. Mazurenko, G. A. Battiston, P. Zanella, F. Tisato, F. Braga, P. Traldi, *Appl. Organomet. Chem.* **1995**, 9, 259.
- [22] G. Carta, G. Rossetto, S. Sitran, P. Zanella, L. Crociani, K. V. Zherikova, N. B. Morozova, N. V. Gelfond, P. P. Semyannikov, L. V. Yakovkina, T. P. Smirnova, I. K. Igumenov in *Chemical Vapor Deposition: Proc. EUROCVD-15* (Eds. A. Devi, H. Parala, M. L. Hitchman, R. A. Fischer, M. D. Allendorf), The Electrochemical Soc., Pennington, NJ **2005**, Vol 05-09, p. 260.
- [23] G. Carta, N. El. Habra, G. Rossetto, L. Crociati, G. Torzo, P. Zanella, G. Cavinato, G. Pace, S. Kaciulis, A. Mezzi, submitted to *Thin Solid Films*. vPlease updatev
- [24] G. Chandra, M. F. Lappert, *J. Chem. Soc.* **1968**, 1940.
- [25] S. Codato, G. Carta, G. Rossetto, G. A. Rizzi, P. Zanella, P. Scardi, M. Leoni, *Chem. Vap. Deposition*, **1999**, 5, 159.
- [26] D. D. Sarma, C. N. R. Rao, *J. Electron. Spectrosc. Relat. Phenom.* **1980**, 20, 25.
- [27] R. Anwender, F. C. Munck, T. Priermeier, W. Scherer, O. Runte, W. A. Herrmann, *Inorg. Chem.* **1997**, 36, 3545.